

Raman and infrared study of phase transitions in solid HBr under pressure

E. Katoh

Core Research for Evolutional Science and Technology, Japan Science and Technology Corporation, Kawaguchi, Saitama 332-0012, Japan

H. Yamawaki, H. Fujihisa, M. Sakashita, and K. Aoki*

National Institute of Materials and Chemical Research, Tsukuba, Ibaraki 305-8565, Japan
and Core Research for Evolutional Science and Technology, Japan Science and Technology Corporation, Kawaguchi, Saitama 332-0012, Japan

(Received 3 December 1998)

Phase transition in solid HBr has been investigated by Raman and infrared spectroscopy up to 50 GPa at 298 K. The liquid transforms to a cubic structure ($Fm\bar{3}m$) with a bromine fcc lattice at 0.5 GPa and further to an orthorhombic structure ($Cmc2_1$) consisting of zigzag chains of hydrogen-bonded molecules at 13 ± 0.5 GPa. At about 39 ± 2 GPa, Raman peaks related to the molecular stretch and rotation disappear and two lattice peaks remain. The $Cmc2_1$ orthorhombic structure transforms into a $Cmcm$ orthorhombic structure with symmetrized hydrogen bonds. The symmetrized phase is unstable; HBr molecules begin to dissociate after the bond symmetrization and Br_2 molecules are formed. [S0163-1829(99)08917-1]

INTRODUCTION

Hydrogen halides, HX ($X = F, Cl, Br,$ and I), are diatomic molecules forming hydrogen bonds in a condensed state. Three crystalline phases are known to exist at low temperatures and ambient pressure.¹⁻³ The lowest temperature phase (phase III), for example, of HBr has an orthorhombic $Cmc2_1$ structure consisting of the planar zigzag chains of molecules connected by hydrogen bonds. The molecular chains run along the crystalline c axis on the planes parallel to the bc plane, being separated from the adjacent chains by van der Waals forces as drawn in Fig. 1. The orthorhombic crystal is a ferroelectric insulator as can be seen from dipole ordering in the direction parallel to the crystalline c axis. The temperature elevation in phase III induces phase transitions to phase II at 90 K and to phase I at 114 K. The phase II has an orthorhombic $Cmca$ structure with protons in twofold disordered positions around Br atoms. In phase I, Br atoms construct a face-centered-cubic lattice ($Fm\bar{3}m$) with completely disordered protons occupying one of twelve equivalent sites. The same or similar structural sequence has been observed for HCl and HI, whereas only $Cmc2_1$ orthorhombic structure is known for HF.

Few high pressure experiments have been reported for hydrogen halides in spite of the simplicity of molecular and crystal structures. Brillouin and Raman scattering spectra of HF(DF) have been measured for single crystals of the $Cmc2_1$ orthorhombic structure to 12 GPa.^{4,5} Disappearance of the molecular stretching peaks and change in the librational peak positions at about 6 GPa suggested a phase transition to a symmetric hydrogen-bonded phase. Far-infrared absorption spectra have been measured for the $Cmc2_1$ orthorhombic phases of HCl and HBr to 0.5 GPa at 4.2 K.⁶ The observed translational and librational frequencies were compared with those calculated using empirically determined intermolecular potentials. Raman measurements beyond 10 GPa at 100 K have been reported for HCl and HBr by Johannsen.⁷ The spectra of HBr revealed a phase transition

in the orthorhombic phase at about 32 GPa possibly in association with hydrogen bond symmetrization. No phase transition was observed for the orthorhombic phase of HCl up to 40 GPa. A phase study of HBr in a temperature range of 20–300 K and a pressure range to 20 GPa has recently been made by Raman measurement, determining precisely the boundaries among the known phase I, II, III and a newly observed phase I'.⁸ Although hydrogen bond symmetrization has been reported for HF and HBr as described above, more detailed investigations on them are required for an understanding of the symmetrization mechanism.

We have measured Raman scattering and infrared (IR) absorption spectra for solid HBr at pressures up to 50 GPa at 298 K. The purpose was to investigate phase transition and change in hydrogen bonding state in such a simple molecular solid. Applying pressure was expected to cause successive phase transitions as observed at low temperatures and furthermore molecular dissociation with hydrogen bond symmetrization at a sufficiently high pressure. Raman and infrared measurements provided complementary information on

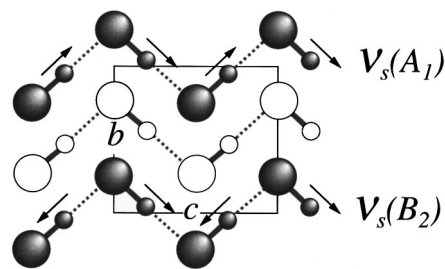


FIG. 1. Molecular arrangement in the bc plane of the orthorhombic $Cmc2_1$ structure, phase III, of solid HBr. Solid and open circles indicate molecules located at $a=0$ and $\pm 1/2$, respectively. The proton displacements associated with a symmetric $\nu_s(A_1)$ and an antisymmetric stretching vibration $\nu_s(B_2)$ are presented with arrows along the upper and lower zigzag chains, respectively. The hydrogen bonds are symmetrized by putting the protons (small spheres) at the midpoints between the bromine (large spheres) neighbors.

the vibrational state, allowing a detailed discussion on the nature of phase transitions observed.

EXPERIMENT

High pressure Raman spectra were measured with a diamond anvil cell (DAC) at 298 K. Sample preparation and loading in the DAC were carried out in a glove box purged with nitrogen gas. HBr gas (stated purity 99.9%) was conducted with a flexible teflon tube inside the DAC and solidified in a small sample chamber made by drilling a $80\ \mu\text{m}$ hole on a rhenium metal sheet $60\ \mu\text{m}$ in thickness. The DAC was cooled with liquid nitrogen below the melting temperature of 185 K in order to solidify the conducted gas immediately on the gasket. Rhenium was chemically inactive with HBr acid. The 488 nm line of an Ar-ion laser was used for Raman excitation. Scattered lights from the sample were analyzed with a single monochromator with a band-reject filter placed in front of the entrance slit of the monochromator to block the excitation laser lights. Spectra were recorded with a charge-couple-device (CCD) detector capable of covering a wave number region of $3000\ \text{cm}^{-1}$ at once with a spectral resolution of $2.3\ \text{cm}^{-1}$. The excitation laser light having a roughly estimated power of 10 mW was defocused to about $80\ \mu\text{m}$ in diameter on the sample surface in order to avoid possible radiation damage of the sample. The pressure was determined on the basis of the ruby scale.⁹

IR absorption spectra were measured for thick and thin samples with a small DAC. A thick sample was prepared by pushing solidified HBr into a $70\ \mu\text{m}$ diameter and $30\ \mu\text{m}$ thick chamber made in a rhenium gasket. A thin film was prepared by deposition of HBr gas onto the surface of a metal gasket packed with a pressure medium of KBr fully in its sample space. The film was pressurized between the diamond and KBr medium. Thin diamond anvils of 1.2 mm thickness were employed to obtain absorption spectra over the whole measuring wave number region including absorption bands due to the diamonds, allowing pressure generation to a rather low pressure of about 35 GPa. Pressure generation beyond 35 GPa was achieved using 1.5 mm thick anvils at the cost of spectral measurement in the diamond absorption region. The absorption spectra were taken with a microscope FT-IR spectrometer for a wavenumber region from 700 to $5000\ \text{cm}^{-1}$ with a selected spectral resolution of $4\ \text{cm}^{-1}$.

Measured Raman and IR spectra were corrected for emission or absorption from the diamond anvils. Diamond exhibits the first order Raman peak at $1333\ \text{cm}^{-1}$ and second one at about $2450\ \text{cm}^{-1}$. A reference Raman spectrum was taken by moving slightly a focusing position of the excitation light from the sample to the gasket surface. The spectrum thus measured was used to subtract the diamond peaks from the raw spectrum and this correction was made at every measuring pressure point. IR absorption peaks of diamond appear in the frequency region from 1700 to $2600\ \text{cm}^{-1}$. Reference spectra was measured in advance for an empty DAC containing only a pressure medium of KBr in the gasket hole at a pressure interval of about 3 GPa up to 50 GPa. The diamond absorption was successfully removed from the raw spectrum by choosing an appropriate reference spectrum measured at a corresponding pressure.

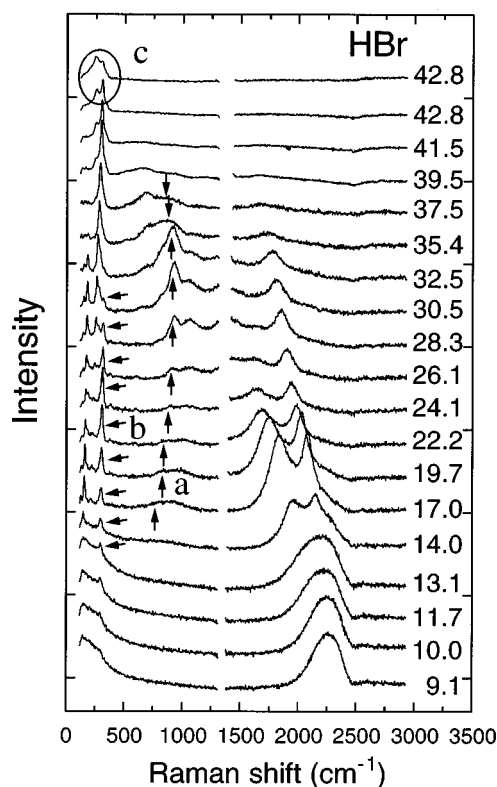


FIG. 2. Raman spectra of solid HBr measured to 43 GPa at 298 K. The inserted numerical values represent pressures in GPa. The I–III phase transition occurs at 13 GPa with a peak splitting of the stretching mode located around $2000\ \text{cm}^{-1}$ and appearance of the librational and lattice modes. The stretching and librational peaks disappear above 39 GPa and the lattice peak with a shoulder newly appeared in the low frequency side remains. Spectral change with time is observed in the top spectrum measured after 24 h from pressure increase to 42.8 GPa. Arrow *a*: one librational peak showing Fermi resonance. Arrow *b*: the peak of Br_2 included as impurity. Circle *c*: spectral change with time at 42.8 GPa.

RESULTS

Figure 2 shows the Raman spectra of HBr measured up to 43 GPa. HBr molecule itself has only one intramolecular or stretching vibration. One broad peak observed around $2200\ \text{cm}^{-1}$ at 13.1 GPa was hence assigned as the stretching mode. The stretching peak split into a doublet at about 13 GPa. In association with the peak splitting, several peaks appeared in the lattice vibrational region below $1000\ \text{cm}^{-1}$. The peaks around $900\ \text{cm}^{-1}$, which were observed as a weak broad peak at low pressures, were assigned as librational modes, while those below $300\ \text{cm}^{-1}$ as translational lattice modes. The splitting stretch peaks showed shift to low frequency and especially the shift of the lower frequency peak was very rapid. The librational peaks showed unusual pressure behavior. One librational peak at $836\ \text{cm}^{-1}$ (arrow *a*) in the 19.7 GPa spectrum, for instance, moved initially to high frequency, turning to shift toward low frequency at about 30 GPa. The peak intensity changed from increasing to decreasing also at about 30 GPa. Every translational lattice peak moved little to high frequency.

Slight changes in spectra accompanied by phase transitions were observed at about 39 and 43 GPa. The Raman peaks related to the molecular stretch and libration became

weakened with increasing pressure and disappeared at about 40 GPa eventually, while the translational lattice peaks remained with slight changes in peak position and intensity. The 39.5 GPa spectrum showed one strong peak at 289 cm^{-1} . A slight increase in pressure produced a new peak in the low frequency side of the original peak which showed a gradual decrease in peak intensity. Their peak positions were 256 and 305 cm^{-1} at 42.8 GPa . No peak was observed in the intramolecular vibrational region. Careful observation revealed that the lattice vibrational spectrum changed gradually with time. The spectrum measured after keeping the pressure at 42.8 GPa for 24 h showed an inversion in peak intensity and a slight shift in the low-frequency peak position. These spectral changes were found to be due to dissociation of HBr molecules and subsequent formation of Br_2 molecules.

A peak steadily remaining at 300 cm^{-1} would arise from Br_2 molecules involved in the original gas sample as impurity. The peak (arrow *b* in Fig. 2), whose position was in agreement with that of the stretching vibration of Br_2 in an orthorhombic structure,¹⁰ grew up to 22 GPa and disappeared at about 32 GPa . This intensity change does not merely imply an increase or decrease in Br_2 amount but can be interpreted as a resonance Raman effect. Raman intensity is significantly enhanced for an excitation light having a photon energy comparable to an electronic transition energy or band gap energy. The resonance probably occurred at about 22 GPa in solid Br_2 for the excitation with the 488 nm light, resulting in an intensity enhancement selectively for the Raman peaks from Br_2 molecules. In order to estimate the amount of solid Br_2 , we measured x-ray diffraction patterns for the pressurized solid HBr. No peak from solid Br_2 was detected even at pressures around 22 GPa where the Raman signal became most intense. The amount of Br_2 impurity contained in HBr solid was roughly estimated to be less than 0.1% in volume ratio.

Typical IR spectra measured for thin and thick samples are shown in Figs. 3(A) and 3(B), respectively. The stretching peak exhibited very strong absorption and the whole peak shape was obtained for the thin film [Fig. 3(A)]. A peak splitting was observed at about 13 GPa in good agreement with the Raman results. The doublet peaks merged into one asymmetric broad peak with increasing pressure and collapsed above 30 GPa . The IR spectra of the thick sample showed an extremely saturated stretching peak in the frequency region from 1500 to 2500 cm^{-1} . It barely showed a tendency to shift toward low frequency with peak broadening. Above 14 GPa four peaks newly appeared in the low frequency side of the stretching peak again in agreement with the Raman results. They were located at 710 , 841 , 967 , and 1357 cm^{-1} in the spectrum taken at 20.4 GPa and assigned as the librational vibrations of HBr molecules.⁶ On further compression, absorption developed in the low frequency region and then extended to the high frequency region, covering the whole measuring region as shown in the top spectrum taken at 47.5 GPa . The librational peaks were able to be measured to 25 GPa .

The peak frequencies obtained from the observed Raman and infrared spectra are plotted as a function of pressure in Fig. 4. The spectral changes at about 13 GPa are explained by I-III ($Fm3m$ cubic; $Cmc2_1$ orthorhombic) transition as

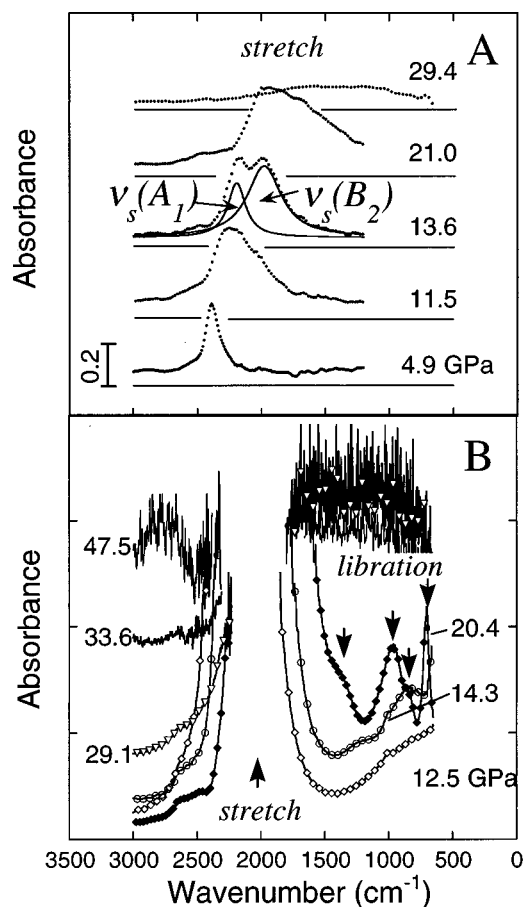


FIG. 3. Infrared absorption spectra of solid HBr measured for the thin film (A) and thick sample (B). In (A), the spectra are shifted with 0.3 -unit increments in the vertical direction. No shift is made in (B). The I-III transition is observed at about 13 GPa in good agreement with the Raman results.

discussed later in detail. Mode assignment of Raman and infrared peaks can hence be made on the basis of those reported in the low temperature Raman and infrared measurements.^{11,12} Four fundamental librational modes, $\nu_L(A_2)$, $\nu_L(B_2)$, $\nu_L(A_1)$, and $\nu_L(B_1)$, are predicted for the

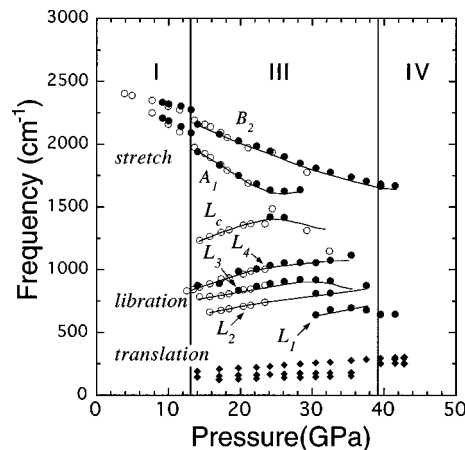


FIG. 4. The variation of vibrational frequencies with pressure measured for solid HBr. Solid and open symbols represent the peak frequencies obtained by Raman scattering and infrared absorption measurement, respectively. Fine solid lines are guides to eyes.

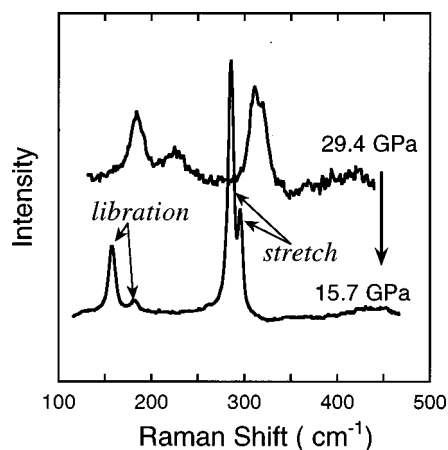


FIG. 5. Raman spectra measured for solid HBr on unloading process. The observed four peaks are assigned as the stretching and librational modes of solid Br_2 having an ordinary $Cmca$ orthorhombic structure.

$Cmc2_1$ orthorhombic structure of phase III. However, the symmetry assignments of these modes are still inconclusive and so here the observed peaks are labeled L_1 , L_2 , L_3 and L_4 in order to increasing frequency. A peak additionally observed at about 1200 cm^{-1} just after I-III transition is assigned as a combination of the librations L_c . The Raman peak of diamond around 1333 cm^{-1} overlaps this combination peak, interfering with the observation of the L_c peak in the low pressure region. This missing peak can be measured by IR absorption and the observed infrared frequencies are shown to connect smoothly with the Raman frequencies at about 24 GPa. The variation of the combination frequency is thus obtained for the whole pressure region measured. The IR data are shown to complement those obtained by Raman measurement for the fundamental librational modes as well. The phase III transforms to another high pressure phase labeled IV at about 39 GPa.

The high pressure behavior of the stretching modes is very similar between phases I and III. The peak of phase I has an asymmetric shape with a shoulder in the low frequency side (see Raman and IR spectra given in Figs. 2 and 3), being well fitted with two Lorentzian peaks. They show frequency decreases at different rates and consequently the peak splitting becomes large as the pressure is increased in phase I. The tendency of frequency variation continues in phase III after the transition at 13 GPa accompanied by a frequency drop by about 80 cm^{-1} . The $\nu_s(B_2)$ stretching frequency decreases monotonically to 39 GPa, while the $\nu_s(A_1)$ stretching mode shows a more rapid decrease up to 22 GPa and interactions with other vibrational modes at higher pressures. Such interaction is known as Fermi resonance,^{13,14} modifying the frequencies and Raman intensities as the results of vibrational mode mixing. The resonance is observed for the L_c combination and L_3 modes. The modified frequencies are shown to avoid to cross as clearly seen between the $\nu_s(A_1)$ and ν_{L_c} around 26 GPa.

Raman spectra measured at 29.4 and 15.7 GPa during pressure releasing from 43 GPa are shown in Fig. 5. These spectral features are different from those measured for solid HBr at the corresponding pressures on loading process, losing spectral features in the librational and stretching vibra-

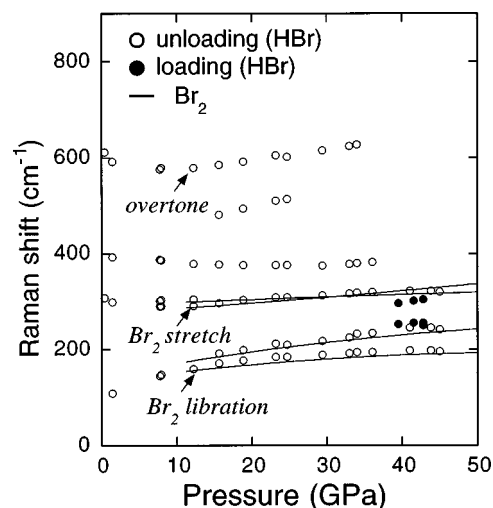


FIG. 6. Open circles represent Raman peak frequencies measured for the dissociated phase of solid HBr on unloading process. Solid circles are those measured for solid HBr on loading process. Solid lines represent Raman frequencies of solid Br_2 reported in Ref. 9. The Raman peak around 600 cm^{-1} is assigned as the overtone of the stretching mode of Br_2 . The remaining two peaks are not identified.

tional regions. The Raman peaks appear only in the lattice vibrational region around 160 and 300 cm^{-1} at 15.7 GPa. They are interpreted as the stretching and librational vibrations of Br_2 in a $Cmca$ orthorhombic structure.¹⁰ The frequencies measured on unloading process are plotted along with those reported for the orthorhombic phase of solid Br_2 measured on loading process in Fig. 6. They are on the same lines, indicating conversion from HBr to Br_2 molecules via the high pressure phase IV. In the IR spectra, the chemical reaction associated with dissociation of HBr molecules was also observed. Spectra were measured for the specimen pressurized to 50 GPa while the pressure was gradually released to ambient pressure. No absorption peak was recovered in the molecular stretching region around 2300 cm^{-1} even at sufficiently low pressures below 10 GPa.

DISCUSSION

Phase transition

A phase transition from $Fm3m$ cubic to $Cmc2_1$ orthorhombic structure occurs at 13 GPa. The Raman spectra of phase I show one broad peak at about 2300 cm^{-1} in the intramolecular vibrational region and no peak in the lattice region. The spectral feature is characteristic of molecular solids having disordered structures. The peak broadening of the molecular stretching mode arises from disordering in molecular orientation and the missing of lattice peaks is due to lack of long range order in molecular arrangement. The low temperature phase I has been determined to have a $Fm3m$ cubic structure.¹ The Raman and IR spectra show one broad peak at about 2500 cm^{-1} ,¹⁵ well corresponding to those observed for the high pressure phase existing from 0.5 to 13 GPa. For the $Cmc2_1$ orthorhombic structure with regularly aligned molecules, a vibrational mode analysis predicts two molecular stretching (A_1 , and B_2), four librational (A_1 , B_1 , A_2 , and B_2), and three translational modes (A_1 , A_2 ,

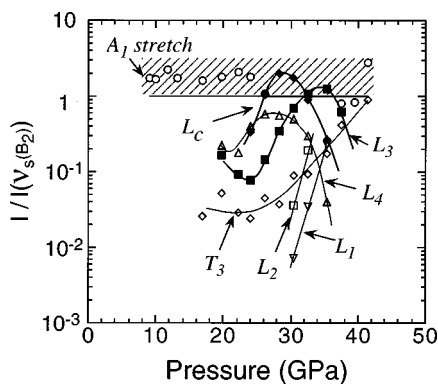


FIG. 7. Relative Raman intensities measured for solid HBr. The ratio I_i/I_0 of each integrated peak intensity I_i to that of the B_2 antisymmetric stretching peak I_0 is plotted as a function of pressure in a logarithmic scale. The resonanced L_c and A_1 librational modes show maxima at 30 and 36 GPa, respectively. The vibrational states in the shaded area can be considered to be an off-resonanced or pure $\nu_s(A_1)$ stretching mode.

and B_2). All of them are Raman active, while those except the translational and librational modes with A_2 symmetry are IR active. The numbers of Raman and IR peaks obtained for the high pressure phase above 13 GPa are in agreement with the prediction. An intermediate phase II, which has been reported to exist for a narrow temperature span of about 2 K around 120 K,³ was not observed at high pressure and 298 K. A recent Raman measurement has proposed presence of another intermediate phase (phase I') between phase I and phase III.⁸ The phase I' has disordered hydrogen bonds and can be distinguished from phase I by the asymmetric peak shape of the stretching mode. Such asymmetry was observed in our Raman and IR measurements as well. However it may be interpreted in terms of instantaneous formation of short chains of HBr molecules in the disordered phase I rather than appearance of a new high pressure phase.¹⁶

The III-IV phase transition at 39 GPa is interpreted in terms of hydrogen bond symmetrization. The $Cmc2_1$ orthorhombic structure can be converted into a symmetrized $Cmcm$ orthorhombic structure by displacing the protons to the midpoints along the hydrogen bonding axes (see Fig. 1). HBr molecules cannot be identified any longer and hence the peaks related to molecular vibrations should disappear. For the $Cmcm$ structure, nine translational lattice modes are predicted based on a vibrational mode analysis. Three of them, A_g , B_{1g} , and B_{3g} , are Raman active. The 39 GPa spectrum with two peaks in the lattice region is in agreement with the prediction although one lattice peak is missing. The transition to $Cmcm$ phase has a second-order or nearly second-order character, showing gradual spectral changes toward the transition pressure of 39 GPa. In other words, the hydrogen bonds are symmetrized continuously in the zigzag chains by compression. Johannsen has reported a possibility of hydrogen bond symmetrization in solid HBr. Their Raman spectra showed disappearance of the stretching peaks and some spectral changes in the lattice vibrational region at about 32 GPa and at 100 K.⁷ The reported peak positions are in agreement with the present results, indicating a transition into the symmetric phase.

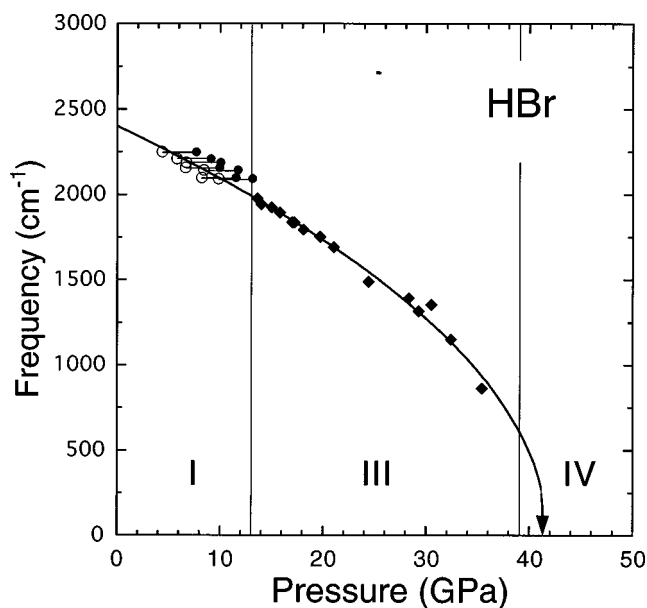


FIG. 8. The variation of the symmetric stretching frequency with pressure. The solid line presents a fitting curve obtained using all the experimental points in phase III. The stretching frequencies of phase I are excluded in the fitting analysis but plotted with an offset of -3.3 GPa for comparison.

The nature of hydrogen bonds in solid HBr seems to be independent on the molecular arrangement but determined roughly by the hydrogen bond length. The structure of phase I consists of disordered protons forming hydrogen bonds with one of twelve equivalent neighboring Br atoms, while that of phase III consists of the infinite planar zigzag chains of hydrogen bonded molecules. The stretching frequency, which is very sensitive to the hydrogen bonding state, shows a very similar pressure dependence in the two phases in spite of the large difference in the molecular arrangement. The decreasing rates of the symmetric stretching frequency, $d\nu_s(A_1)/dp$, are determined to be -29 and -33 $\text{cm}^{-1}/\text{GPa}$ for phase I and phase III, respectively. A 10% decrease in the stretching frequency associated with the I-III transition is mainly due to a corresponding shrinkage in the hydrogen bond length. Formation of infinite hydrogen-bonded molecular chains is likely less responsible for the stretching frequency and the decreasing rate. A frequency decrease of 110 cm^{-1} at the transition corresponds to compression by about 3.3 GPa or offset of -3.3 GPa in the frequency-pressure plotting for phase I. Such offset allows the observed frequencies to be connected smoothly across the I-III transition and them to be fitted with one softening curve (see Fig. 8). The same argument can be applied for the antisymmetric stretching frequency $\nu_s(B_2)$.

Softening of the stretching mode

The hydrogen bond symmetrization process is characterized as a softening of the stretching vibration. Hydrogen bond symmetrization is realized when the protons move to the midpoints between the neighboring Br atoms. This proton displacement will be driven by successive deformation of the proton potential from a double to a single minimum shape. The A_1 symmetric stretching mode in the $Cmc2_1$

structure is described as the collective motions of protons along the hydrogen bonds (Fig. 1) and hence expected to show a softening behavior reflecting the potential deformation predicted. The symmetric stretching frequency shows a rapid decrease in phase III and even in the disordered phase I. The high pressure behavior, however, is largely perturbed owing to the vibrational interactions or resonance effects and observation of the presumed softening behavior is interfered near the symmetrization point.

The unperturbed stretching frequencies are extracted from the perturbed frequencies measured in the resonanced pressure region based on a simple model for Fermi resonance. The A_1 stretching mode would mix with another vibrational mode belonging to the same A_1 symmetry, when the two vibrational frequencies are close sufficiently. The resonanced frequencies and Raman intensities are significantly modified as the results of mode mixing.¹³ The mixing should vanish as the frequencies separate far from each other and hence the unperturbed vibrational states recover eventually. Such resonance behavior is observed for the L_3 fundamental and L_c combination peaks as seen in Fig. 4; consequently the L_3 peak is assigned as the A_1 librational mode and the L_c combination peak most likely as the overtone of it. The pressure dependence of the L_c and A_1 librational frequencies changes from increase to decrease around 25 and 30 GPa, respectively. This is due to mode mixing with the softening A_1 stretching mode.

The librational modes show resonance behavior in Raman intensity as well. The variation of Raman intensity with pressure is plotted for each Raman mode in Fig. 7. The relative intensity of the L_c combination mode increases up to an extrapolated intensity of the A_1 stretching mode drawn as a shaded area at about 25 GPa and then begins to decrease on further compression. The librational mode initially assigned to the L_c combination is thus converted into the A_1 stretching mode around 30 GPa. A similar intensity change is obtained for the A_1 fundamental librational mode showing a maximum intensity at about 36 GPa, where again the A_1 libration is converted into the A_1 stretch. The unperturbed Raman frequencies of the A_1 stretching mode thus obtained are plotted together with those measured at low pressures below 22 GPa and the IR frequencies in Fig. 8. A phenomenological function,¹⁷ $\omega = (\omega_0^2 - ap)^{1/2}$, is applied to fit the stretching frequencies obtained for a pressure range from 14 to 40 GPa, where ω_0 is the frequency at ambient pressure and a the pressure coefficient. The optimized parameters, $\omega_0 = 2401 \text{ cm}^{-1}$ and $a = 1.38 \times 10^5 \text{ cm}^{-2}/\text{GPa}$, reproduce an overall feature of the frequency variation observed, giving an extrapolated critical pressure of 42 GPa for $\omega = 0$. The actual hydrogen-bond symmetrization occurs at 39 GPa slightly lower than the extrapolated pressure.

Molecular dissociation

The phase IV with symmetric hydrogen bonds is unstable, decomposing to form Br_2 molecules. The two Raman spectra measured at 42.8 GPa (see Fig. 2) indicate slight change in the spectral profile with time owing to conversion of HBr molecules to Br_2 ones. Formation of Br_2 molecules is confirmed from Raman spectra measured during pressure releasing. The four Raman peaks are located at the positions exactly same as those reported for solid Br_2 at the corresponding pressures.¹⁰ The separated hydrogen atoms would have to rather form H_2 molecules than remain as radicals, though no Raman signal from the conjectured H_2 molecules was obtained. Solid Br_2 was opaque against the incident laser light, the 488 nm line of an Ar-ion laser, preventing the incident light from going inside the decomposed solid. The effective volume for Raman scattering was largely reduced and probably too small to provide detectable Raman signals of H_2 molecules with much weak Raman scattering intensity compared to Br_2 molecules. No segregation of solid H_2 was found by visual observation with a microscope.

Interchain Br-Br interactions seem to assist dissociation of HBr molecules. The sample changes from colorless transparent to brown in association with the I-III phase transition at 13 GPa. Further compression changes it gradually black and no visible light is transmitted above 40 GPa. This color change is likely attributed to an increase in Br-Br interactions between the parallelly aligned molecular chains. The molecular arrangement of phase III is very similar to that of solid Br_2 ;^{18,19} the $Cmca$ orthorhombic structure of solid Br_2 can be obtained simply by replacing the H atoms with Br in Fig. 1. This molecular arrangement may allow formation of charge transfer interactions between the neighboring HBr molecules, which would be enhanced with increasing pressure or decreasing interchain distance as observed for solid Br_2 .^{18,19} Gradual color change into entirely black by pressure increase up to 40 GPa indicates that the optical absorption edge moves from the visible to infrared region. The strengthening of the interchain bonds, in cooperation with the weakening of the H-Br covalent bonds, is thus considered to be a possible driving force for the molecular dissociation.

SUMMARY

The vibrational spectra indicate two phase transitions at about 13 and 39 GPa. The former transition is interpreted as $Fm3m$ cubic to $Cmc2_1$ orthorhombic transition (I-III transition) and the latter as a second-order or nearly second-order transition associated with hydrogen bond symmetrization (III-IV transition). In addition, HBr molecules are found to dissociate to form Br_2 molecules at about 43 GPa.

*Author to whom correspondence should be addressed.

¹A. Ikram, B. H. Torrie, and B. M. Powell, *Mol. Phys.* **79**, 1037 (1993).

²J. E. Vesel and B. H. Torrie, *Can. J. Phys.* **55**, 592 (1977).

³A. Anderson, B. H. Torrie, and W. S. Tse, *J. Raman Spectrosc.* **10**, 148 (1981).

⁴J. Obriot, F. Fondere, Ph. Marteau, and M. Allavena, *J. Chem. Phys.* **79**, 33 (1983).

⁵S. A. Lee, D. A. Pinnik, S. M. Lindsay, and R. C. Hanson, *Phys. Rev. B* **34**, 2799 (1986).

⁶D. A. Pinnik, A. I. Katz, and R. C. Hanson, *Phys. Rev. B* **39**, 8677 (1989).

⁷P. G. Johannsen, W. Helle, and W. B. Holzapfel, *J. Phys. C* **8**, 199 (1984).

⁸T. Kume, T. Tsuji, S. Sasaki, and H. Shimizu, *Phys. Rev. B* **58**, 8149 (1998).

- ⁹H. K. Mao, J. Xu, and P. W. Bell, *J. Geophys. Res.* **91**, 4673 (1986).
- ¹⁰Y. Akahama, H. Kawamura, H. Fujihisa, K. Aoki, and Y. Fujii, *Rev. High Pressure Sci. Technol.* **7**, 793 (1998).
- ¹¹M. Ito, M. Suzuki, and T. Yokoyama, *J. Chem. Phys.* **50**, 2949 (1969).
- ¹²R. Savoie and A. Anderson, *J. Chem. Phys.* **44**, 548 (1966).
- ¹³K. Aoki, H. Yamawaki, and M. Sakashita, *Science* **268**, 1322 (1995).
- ¹⁴V. V. Struskin, A. F. Goncharov, R. J. Hemley, and H. K. Mao, *Phys. Rev. Lett.* **78**, 4446 (1997).
- ¹⁵L. C. Brunel and M. Peyron, *C. R. Seances Acad. Sci., Vie Acad.* **264**, 930 (1967).
- ¹⁶T. Ikeda, M. Sprik, K. Terakura, and M. Parrinello, *Phys. Rev. Lett.* **81**, 4416 (1998).
- ¹⁷Ph. Pruzan, *J. Mol. Struct.* **322**, 279 (1994).
- ¹⁸Y. Fujii, K. Hase, Y. Ohishi, H. Fujihisa, N. Hamaya, K. Takemura, O. Shimomura, T. Kikegawa, Y. Amemiya, and T. Matsushita, *Phys. Rev. Lett.* **63**, 536 (1989).
- ¹⁹H. Fujihisa, Y. Fujii, K. Takemura, and O. Shimomura, *J. Phys. Chem. Solids* **56**, 1439 (1995).